Increased aridity in southwestern Africa during the warmest periods of the last interglacial

D.H. Urrego[1,2]*, M.F. Sánchez Goñi[1], A.-L. Daniau[3], S. Lechevrel[4], V. Hanquiez[4]

[1] Ecole Pratique des Hautes Etudes EPHE, Université de Bordeaux, Environnements et

Paléoenvironnements Océaniques et Continentaux (EPOC), Unité Mixte de Recherche 5805, F-

33615 Pessac, France.

[2] Geography, College of Life and Environmental Sciences, University of Exeter, United Kingdom.

[3] Centre National de la Recherche Scientifique CNRS, Université de Bordeaux, Environnements et

Paléoenvironnements Océaniques et Continentaux (EPOC), Unité Mixte de Recherche 5805, F-

33615 Pessac, France.

[4] Université de Bordeaux, Environnements et Paléoenvironnements Océaniques et Continentaux

(EPOC), Unité Mixte de Recherche 5805, F-33615 Pessac, France.

*Corresponding author full address: Geography, College of Life & Environmental Sciences, University

of Exeter, Amory Building B302, Rennes Drive, EX4 4RJ, Exeter, United Kingdom. E-mail:

d.urrego@exeter.ac.uk. Tel: +44 (0)1392 725874, Fax: +44 (0)1392 723342.

21 **Abstract**

22   Terrestrial and marine climatic tracers from marine core MD96-2098 were used to

23 reconstruct glacial-interglacial climate variability in southwestern Africa between 194 and 24

24 thousand years before present. The pollen record documented three pronounced expansions of

25 Nama-Karoo and fine-leaved savanna during the last interglacial (Marine Isotopic Stage 5 – MIS 5).

26 These Nama-Karoo and fine-leaved savanna expansions were linked to increased aridity during the

27 three warmest substadials of MIS 5. Enhanced aridity potentially resulted from a combination of

28 reduced Benguela Upwelling , expanded subtropical high-pressure cells, and reduced austral-

29 summer precipitation due to a northward shift of the Intertropical Convergence Zone. Decreased

30 austral-winter precipitation was likely linked to a southern displacement of the westerlies. In

31 contrast, during glacial isotopic stages MIS 6, 4 and 3, Fynbos expanded at the expense of Nama-

32 Karoo and fine-leaved savanna indicating a relative increase in precipitation probably concentrated

33 during the austral winter months. Our record also suggested that warm-cold or cold-warm

34 transitions between isotopic stages and substages were punctuated by short increases in humidity.

35 Increased aridity during MIS 5e, 5c and 5a warm substages coincided with minima in both

36 precessional index and global ice volume. On the other hand, austral-winter precipitation increases

37 were associated with precession maxima at the time of well-developed northern-hemisphere ice

38 caps.

39

40 **Key words**

41 Benguela upwelling, fine-leaved savanna, Intertropical Convergence Zone (ITCZ), last interglacial,

42 Nama-Karoo, southern westerlies, southwestern Africa.

43

44 **1. Introduction**

45   Southern Africa is influenced at present by tropical and subtropical atmospheric circulation

46 and by both the Indian and the Atlantic Oceans (Tyson and Preston-Whyte, 2000). The water

47   exchange between the two oceans is termed the Agulhas leakage and is suggested as a potential

48   trigger of meridional overturning circulation changes (Beal et al., 2011; Biastoch et al., 2008). The

49   Benguela Upwelling System (BUS) also affects climate in southwestern Africa and is linked to arid

50   conditions on the continent (Lutjeharms and Meeuwis, 1987). The complex link between globally-

51   important atmospheric and oceanic systems and the climate of southern Africa make understanding

52   past climate change in the region particularly significant.

53   Whether southern Africa was characterised by aridity or by increased humidity during the

54   last interglacial remains unclear. Previous work using planktic foraminifera assemblages has

55   documented an intensification of the Agulhas leakage during interglacials (Peeters et al., 2004),

56   which suggests a reduced influence of the subtropical front and reduced precipitation. Other works

57   have shown increased sea surface temperatures (SST) in the Benguela Current during interglacials

58   linked to weakening of BUS (Kirst et al., 1999). Additionally, decreased influence of the Intertropical

59   convergence zone (ITCZ) has been suggested for southern Africa during interglacials (Tyson, 1999)

60   pointing to its northward migration. These three climatic factors combined would result in a slight

61   increase in humidity in northeastern South Africa during interglacials. However, other works suggest

62   contrasting climate conditions with increased interglacial aridity based on ratios of aeolian dust and

63   fluvial mud in marine sediments off southern Africa (Stuut and Lamy, 2004).

64   Vegetation-based climate reconstructions for southern Africa have been less straight

65   forward given the paucity of records (Dupont, 2011) and fragmentary nature of some terrestrial

66   sequences (Scott et al., 2012; Meadows et al., 2010). On one hand, some records point to

67   expansions of the Fynbos biome (Shi et al., 2001) and the winter-rainfall zone during glacial periods

68   (Chase and Meadows, 2007), and to a contracting Namibian Desert during interglacials (Shi et al.,

69   2000) and the late Holocene (Scott et al., 2012). On the other hand, it has been suggested that

70   savannas expanded southwards during the Holocene climate optimum (Dupont, 2011), and that the

71   southern Africa summer-rainfall zone expanded during interglacials due to a strengthening of the

72   Walker circulation and a southward migration of the ITCZ (Tyson, 1999). Contrastingly, significant

73   reductions of austral-summer precipitation in southern Africa are suggested to coincide with

74   precession minima both during glacials and interglacials (Partridge et al., 1997), and are

75   independently supported by reductions of grass-fuelled fires in the subcontinent (Daniau et al.,

76   2013). The latter observations suggest aridity increase and savanna biome reductions, instead of

77   expansions, during the last interglacial precession minima. Whether the last interglacial was

78   characterised by orbitally-driven increased aridity or increased precipitation may have significant

79   implications for resource availability and climate in the region today and in the near future.

80   Projected patterns of precipitation change for the end of the 21st century indicate at least a 20%

81   reduction of precipitation in southern Africa compared to pre-2005 values (IPCC, 2014).

82   Understanding glacial-interglacial climate and vegetation dynamics in this region may help unravel

83   how much of the projected precipitation change corresponds natural variability.

84   In this study we aim to disentangle the contrasting hypotheses of orbital-scale climate

85   change in southern Africa by combining terrestrial and marine tracers from the marine sequence

86   MD96-2098. We use pollen and charcoal as terrestrial tracers, and $\delta^{18}O$ from benthic foraminifera as

87   a marine tracer. Vegetation reconstructions from marine records have contributed to our

88   understanding of ocean-land interactions in many regions of the world, including the Iberian

89   Peninsula (Sánchez Goñi et al., 2000), the eastern subtropical Pacific (Lyle et al., 2012), and the

90   tropical Atlantic (González and Dupont, 2009). Studies from the African margin (e.g. Dupont (2011);

91   Dupont and Behling (2006); Hooghiemstra et al. (1992); Leroy and Dupont (1994); Lézine and

92   Hooghiemstra (1990)) have demonstrated that pollen records from marine sequences are reliable

93   and useful tools to reconstruct changes in the regional vegetation of adjacent landmasses and the

94   climate dynamics at orbital and suborbital timescales. In arid environments, marine sequences are

95   particularly essential in providing continuous records of vegetation change at the regional scale.

96   The pollen sequence from MD96-2098 presented here covers the period between 24 and

97   190 thousand years before present (ka) and provides an integrated picture of past regional

98   vegetation changes in southwestern Africa. Southwestern Africa refers here to the western half of

99   South Africa and Namibia that is drained by the Orange River. We compare vegetation-based

100   atmospheric changes with independent climatic markers from the same marine sequence, along

101   with other regional records for oceanic conditions and global ice dynamics, to reconstruct

102   atmospheric and oceanic configurations around southern Africa for MIS 6, 5, 4 and 3.

103

104   **2. Modern environmental setting**

105   The southwestern part of the African continent (Atlantic side) is influenced by the seasonal

106   migration of the subtropical front and the southern westerlies that bring precipitation during the

107   austral-winter months (Beal et al., 2011). Precipitation in southwestern Africa is additionally

108   controlled by the cold Benguela current and wind-driven upwelling that results in aridity on the

109   adjacent continent (Stuut and Lamy, 2004). In the Indian Ocean, warm waters from the Agulhas

110   current (Beal and Bryden, 1999) and austral-summer heat enhance evaporation and result in

111   relatively high precipitation in southeastern Africa and the interior of the continent (Fig.1). Austral-

112   summer precipitation is also linked to the position of tropical low pressure systems (e.g. ITCZ) and

113   reduced subtropical high pressure (Tyson and Preston-Whyte, 2000). As tropical low-pressure

114   systems migrate northwards during the austral winter, subtropical high pressure significantly

115   reduces austral-summer precipitation in southern Africa. This climatic configuration broadly

116   determines the vegetation distribution in southern Africa.

117   The vegetation of southern Africa was initially classified into phytogeographical regions

118   (White, 1983; Goldblatt, 1978), and later revisited and described into seven biome units (Rutherford,

119   1997). These include the Succulent-Karoo, Nama-Karoo, Desert, savanna, Fynbos, Grassland, and

120   forest (Fig.1). The Succulent-Karoo receives between 20 and 290 mm/yr of which more than 40%

121   falls during the austral-winter months (Rutherford, 1997). The two most abundant succulent families

122   are Crassulaceae and Mesembryanthemaceae, and non-succulents are Anacardiaceae, Asteraceae,

123   and Fabaceae (Milton et al., 1997). C4 perennial grasses (Poaceae) have relatively low abundance in

124   the Succulent-Karoo (Milton et al., 1997).

125   The Nama-Karoo receives precipitation from 60 to 400 mm/yr falling primarily during the

126   austral summer (Palmer and Hoffman, 1997). Vegetation is characterized as dwarf open shrubland

127   with high abundance of Poaceae, Asteraceae, Aizoaceae, Mesembryanthemacae, Liliaceae and

128   Scrophulariaceae (Palmer and Hoffman, 1997). Grasses from the Poaceae family can be particularly

129   dominant in the Nama-Karoo biome (Fig.2a). The Nama- and Succulent-Karoo are structurally similar

130   but influenced by different seasonal precipitation (Rutherford, 1997). The Nama-Karoo is influenced

131   primarily by austral summer precipitation, while the distribution of the Succulent-Karoo coincides

132   with the austral-winter rainfall region (Chase and Meadows, 2007). To the northwest, the Nama-

133   Karoo biome transitions into the Desert, where mean annual precipitation can be as low as 20

134   mm/yr (Jürgens et al., 1997) and water deficit as high as 2000 mm (Barnard 1998, Fig.1d). The Desert

135   reaches 300 km inland and its low precipitation input is linked to the intensity of BUS (Cowling et al.,

136   1994).

137   High precipitation seasonality (i.e. difference between dry-season and rainy-season

138   precipitation) and high austral-summer rainfall characterize the savanna. The savanna biome

139   represents a mosaic that includes shrublands, dry forests, lightly-wooded grasslands, and deciduous

140   woodlands (Scholes, 1997). At the landscape scale however, the savanna can be subdivided into the

141   fine- and broad-leaved savannas based on moisture conditions and soils (Scholes, 1997). The fine-

142   leaved savanna (Fn-LSav) is found in dry and fertile environments (between 400 and 800 mm/yr),

143   and the broad-leaved savanna (Bd-LSav) is found in nutrient-poor and moist environments (up to

144   1500 mm/yr) (Scholes, 1997). Additionally, in the Fn-LSav fuel load and fire frequency are very low,

145   while Bd-LSav has high fuel load and fire frequency (Scholes, 1997; Archibald et al., 2010). The Fn-

146   LSav is found to the northeast of the Nama-Karoo biome (Fig.1), known as the Kalahari Highveld

147   transition zone (Cowling and Hilton-Taylor, 2009). Due to the transitional character of the Fn-LSav,

148   some of its outer parts have been classified as grassland or Nama-Karoo (White, 1983). The

149   composition of the Fn-LSav can be similar to that of the Nama-Karoo, with dominance of C4 grasses

150   (Poaceae) and succulent plants, but it differs in having scattered trees (Fig.2b) (Cowling et al., 1994).

151   The Bd-LSav is characterized by broad-leaved trees from the Caesalpinaceae and Combretaceae

152   families and an understory dominated by grasses (Scholes, 1997).

153   The grassland biome is dominated by C4 grasses and non-grassy forbs as *Anthospermum* sp.,

154   *Lycium* sp., *Solanum* sp. and *Pentzia* sp. (O'Connor and Bredenkamp, 1997). At the high elevations

155   the biome is dominated by C3 grasses. In the grasslands, precipitation is highly seasonal with mean

156   annual rainfall ranging between 750 and over 1200 mm, falling primarily during the austral-summer

157   months (O'Connor and Bredenkamp, 1997) (Fig.1).

158   The southernmost part of Africa is characterised by the Fynbos biome, a fire-prone

159   vegetation dominated by Ericaceous and Asteraceae shrubs, diverse *Protea* shrubs and trees, and

160   Restionaceae herbs (Cowling et al., 1997a). The Fynbos biome receives relatively high annual

161   precipitation (1200 mm per year) concentrated during the austral-winter months (Rutherford, 1997).

162   The coastal forest biome is found along the eastern coast of the subcontinent and often occurs in

163   small patches with high abundance of *Podocarpus* (Rutherford, 1997). *Podocarpus* patches can also

164   be found in the southeastern part of the Fynbos.

165

166   **3.   Materials and Methods**

167   *3.1 Marine core description and pollen analysis*

168   Pollen analysis was conducted on marine core MD96-2098 (25°36'S, 12°38'E). This giant

169   CALYPSO core was collected during the IMAGES II-NAUSICAA cruise at a 2910-m water depth from

170   the Lüderitz slope in the Walvis Basin, approximately 500 km northwest of the Orange River mouth

171   (Fig.1). The sediments of this 32-m long core were composed of calcium carbonates, biogenic silica,

172   clays and organic matter (Bertrand et al., 1996). The core was sampled every 10 cm between 450

173   and 1940 cm (uncorrected depth) for pollen analysis. The uncorrected depth did not take into

174   account artificial gaps created during piston extraction (Bertrand et al., 1996).

175   Sample volumes were estimated by water displacement. Pollen concentrations per unit

176   volume were calculated based on a known spike of exotic *Lycopodium* spores added to each sample.

177   Pollen extraction techniques included treatment with Hydrofluoric and Hydrochloric acids, and

178   sieving through 150 and 10-µm filters. This filtration allowed separating small non-palynomorph

179   particles and concentrating pollen grains and spores. An independent test of this protocol showed

180   that the use of a 10-µm sieve had no effect on the pollen spectra of marine samples, i.e. comparison

181   of filtered and unfiltered sample counts showed that taxa were not selectively filtered out during

182   pollen preparation and concentration (see http://www.ephe-

183   paleoclimat.com/ephe/Lab%20Facilities.htm for a detailed pollen preparation protocol). Marine

184   sediment samples from MD96-2098 were analysed under the microscope until a sum of at least 100

185   pollen grains excluding fern spores was reached.

186   We used the pollen spectra from 31 terrestrial surface samples collected along a transect

187   (Fig.1) from Cape Town (South Africa) to Lüderitz (Namibia) and designed to cover the four major

188   biomes of southwestern Africa (Table S1). The transect included samples from the Desert, Fynbos,

189   Nama- and Succulent-Karoo. The terrestrial surface samples were treated with standard acetolysis

190   (Faegri and Iversen, 1989) and analysed under the microscope until a pollen sum greater than 300

191   grains was reached. Additional details on terrestrial surface-sample collection and analysis can be

192   found in the Supplementary material. We also used previously-published pollen spectra from 150

193   additional surface samples collected between 22° and 35° latitude south (APD, Gajewski et al. 2002).

194   These pollen spectra were used to assess the distribution of Poaceae pollen abundance and other

195   pollen taxa with potential indicator value for large biomes in southern Africa. ArcGIS 10 was used to

196   draw iso-lines of pollen percentages by interpolating values from a total of 178 surface samples

197   through the natural neighbour method. Additionally, we analysed two marine pollen samples from

198   the upper part of core MD96-2098 (at 5 and 10 cm depth). We compared the pollen spectra from

199   these core top samples with the pollen signal of the modern vegetation to evaluate how well marine

200   sediments represent the vegetation of the adjacent landmasses, and to aid interpretation of the

201   pollen record (see also Lézine and Hooghiemstra 1990).

202   Pollen identification was aided by the pollen reference collection of the Department of Plant

203   Sciences at University of the Free State (Bloemfontein, South Africa), the African Pollen Database

204   (APD) (http://medias3.mediasfrance.org/pollen), the Universal Pollen Collection

205   (http://www.palyno.org/pollen), and pollen descriptions published by Scott (1982). Pollen grains

206   from the Asteraceae family were grouped into three pollen taxa: *Artemisia-type*, *Stoebe*-type and

207   other morphotypes were classified into Asteraceae-other. Some morphotypes were grouped into

208   family types: Acanthaceae, Chenopodiaceae-Amaranthaceae, Crassulaceae, Cyperaceae, Ericaceae,

209   Myrtaceae, Ranunculaceae, Restionaceae, and Solanaceae.

210   Detrended correspondence analysis (DCA) and non-metric multidimensional scaling (NMDS)

211   (McCune and Grace, 2002) were used as parametric and non-parametric ordinations to summarize

212   changes in the fossil pollen record. Results from the DCA ordination were preferred when NMDS was

213   unable to reach a stable solution after several random starts, and when stress levels were too high

214   to allow a meaningful interpretation (McCune and Grace, 2002). These ordinations were performed

215   on the complete dataset and filtering out pollen morphotypes that occurred only in one sample.

216   Results from the ordination performed on the reduced dataset were preferred when differences in

217   axis scores were not discernible between the two ordinations to reduce the statistical effect of rare

218   taxa.

219

220   *3.2 Marine core chronology*

221   Two sediment gaps between 693 and 709 cm and 759 and 908 cm were described in the

222   core log. These gaps were considered artificial and linked to piston extraction (Bertrand et al., 1996),

223   thus the record could be assumed continuous. Depths were corrected to take into account these

224   artificial sediment gaps. An age model was established for the record based on 16 marine isotope

225   events (MIE) from the *Cibicidoides wuellerstorfi* δ^{18}O benthic record of MD96-2098 (Bertrand et al.,

226   2002) and 14 Accelerator Mass Spectrometer radiocarbon ages (AMS ^{14}C) from mixed planktonic

227   foraminifera extracted from MD96-2098 (Table S2). The 14 AMS ^{14}C dates were produced at the

228 Laboratoire de Mesure du Carbone 14. One single ^{14}C date showed an age reversal and was

229 therefore excluded from the chronology on the principle of parsimony. AMS ^{14}C ages were calibrated

230 using the marine09.14c curve (Hughen et al., 2004) from CALIB REV5.0 (Reimer et al., 2013). We

231 applied a 400-year global reservoir correction factor and a weighted mean Delta R of 157 years

232 derived from 9 regional reservoir error values from the Marine Reservoir Correction Dataset (Dewar

233 et al., 2012; Southon et al., 2002). MIE ages were derived from LR04 global stack (Lisiecki and

234 Raymo, 2005) and additional sources (Henderson and Slowey, 2000; Drysdale et al., 2007;

235 Waelbroeck et al., 2008; Masson-Delmotte et al., 2010; Sánchez Goñi and Harrison, 2010) (Fig. S1).

236 Sample ages were calculated using a linear interpolation between AMS ^{14}C ages and MIE using the R

237 package PaleoMAS (Correa-Metrio et al., 2010). The average sedimentation rate of core MD96-2098

238 amounts to 0.01 cm yr^{-1}.

239

240 **4. Results and discussion**

241 *4.1 Pollen preservation and sources in marine core MD96-2098*

242 Pollen sums ranged from 100 to 240 grains (excluding fern spores) in the 141 samples

243 analysed from core MD96-2098. We identified 83 different pollen taxa in the whole sequence, and

244 the mean number of pollen taxa per sample was 21. The proportion of unknown pollen taxa was

245 between 1% and 2% per sample. The total pollen concentration ranged between ca. 300 and 16,000

246 grains/cm^3 during most of MIS 6, 5 and 3 and increased up to 48,000 grains/cm^3 during MIS 4 (Fig.

247 S2). The MIS 5 pollen concentrations were comparable to those found in other oceanic margins

248 (Sánchez Goñi et al., 1999), even though BUS facilitates preservation of pollen grains and other

249 organic microfossils at this site (Bertrand et al., 2003). The low net primary productivity that

250 characterizes the vegetation of southwestern Africa (Imhoff et al., 2004) is probably linked to low

251 pollen production and could explain relatively low pollen concentrations in the continental margin

252 (Fig. S2).

253   Pollen grains are part of the fine sediment fraction and can be transported by two main

254   vectors: aeolian or fluvial (Hooghiemstra et al., 1986; Heusser and Balsam, 1977). Dupont and

255   Wyputta (2003) modelled present-day wind trajectories for marine core locations between 6 and

256   30°S along the coastline of southern Africa. They suggest aeolian pollen input to the Walvis area

257   (23°S) via the southeast trade winds during austral summer, and dominant east-to-west wind

258   directions during the austral fall and winter. These winds transport pollen and other terrestrial

259   particles from the Namib Desert, southern Namibia and western South Africa. The direction of the

260   winds indicate that the Namib Desert, Nama-Karoo and Succulent-Karoo are the most likely sources

261   of pollen in the Walvis Bay area (Dupont and Wyputta, 2003). The authors also infer that south of

262   25°S wind directions are predominantly west to east and aeolian terrestrial input very low. Marine

263   site MD96-2098 is located less than a degree south of the area determined by Dupont and Wyputta

264   (2003) to be dominated by wind-transported terrestrial input. However, given that this threshold

265   was established using only two marine sites located 6° apart at 23°26' (GeoB1710-3) and 29°27'

266   (GeoB1722-1), it is difficult to conclude that MD96-2098 only receives wind-transported pollen.

267   MD96-2098 likely receives fine sediments from the Orange River plume. Sedimentological

268   analyses of the Orange River delta and plume indicate that fine muds are transported both

269   northwards and southwards (Rogers and Rau, 2006). Additionally, an analysis of the imprint of

270   terrigenous input in Atlantic surface sediments found relatively high Fe/K values along the Namibian

271   and South African margin that could reflect the input of Orange River material (Govin et al., 2012).

272   Pollen grains are hence likely to reach the coring site from the Orange River catchment area.

273   Scott et al. (2004) argue that pollen in marine sediments can be the result of long-distance

274   transport by ocean currents, suggesting that pollen assemblages in marine sediments do not reflect

275   accurately past changes in vegetation and climate. However, the highest pollen influx in marine

276   sediments along this margin is near the coast and the vegetation source (Dupont et al., 2007), not

277   along the paths of oceanic currents (i.e. Benguela Current). Additionally, analyses of pollen transport

278   vs. source in northwestern Africa show that pollen grains can sink rapidly in the water column

279 (Hooghiemstra et al., 1986) before they can be carried away by ocean currents. As a result, influence

280 of oceanic currents on the composition of pollen assemblages is probably negligible. Overall, the

281 marine site MD96-2098 might receive both aeolian and fluvial pollen input from the vegetation

282 located east and southeast to the site.

283   The pollen spectra of the two core-top samples from core MD96-2098 are dominated by

284 Poaceae (30 and 40%), Cyperaceae (20%) and Chenopodiaceae-Amaranthaceae (20 and 30%) (Fig.

285 S2). This composition corresponds well with the pollen spectra from the three major biomes

286 occupying today the adjacent landmasses (Fig.1a): Desert, Nama-Karoo and Fn-LSav (Fig. S3). Pollen

287 percentages from Fynbos taxa are less than 10%, *Podocarpus* is weakly represented, and taxa

288 specifically found in the broad-leaved savanna (e.g. Caesalpinaceae, Combretaceae) are not

289 recorded. These results support the assumption that the main pollen source for marine core MD96-

290 2098 is the vegetation from southwestern Africa.

291

292 *4.2 Distribution and interpretation of Poaceae pollen in terrestrial and marine surface samples*

293   Occurrence of Poaceae pollen in all surface samples corresponds to the presence of grass

294 species in virtually all southern African biomes (Cowling et al., 1997b). Altogether, the spatial

295 distribution of Poaceae pollen percentages appears to be essential information to distinguish the

296 pollen signal from major biomes, and therefore climatic zones, in this region. In the eastern and

297 northeastern part of southern Africa, the highest percentages of Poaceae pollen (up to 90%) are

298 found in the pollen rain of the Bd-LSav and grasslands. In the western half of southern Africa,

299 Poaceae pollen percentages in terrestrial surface samples are up to 60% in the Nama-Karoo and its

300 transition with the Fn-LSav (Fig.3). This suggests an overrepresentation of Poaceae in the pollen rain

301 of the Nama-Karoo biome where grasses can be abundant but are not necessarily dominant.

302   Poaceae is likely to be well represented in other parts of the Fn-LSav, but the paucity of

303 surface samples from this biome hinder drawing further conclusions. In the Namib Desert where the

304　　proportion of grasses in the vegetation is low, Poaceae pollen percentages are as high as 25% in

305　　terrestrial surface samples, comparable to 20% reported from hyrax dung (Scott et al., 2004).

306　　　　　In marine surface samples along the southwestern African coast, Poaceae pollen

307　　percentages are as low as 10% in samples collected offshore the Bd-LSav at around 15°S (Fig.3).

308　　Poaceae pollen percentages increase to the south and the highest values (40%) are found between

309　　20 and 25°S (Dupont and Wyputta, 2003) and correspond well with the distribution of the Desert

310　　and the Fn-LSav on the continent. The Poaceae pollen percentages in the two core-top samples from

311　　MD96-2098 are used to extend the iso-lines drawn by Dupont and Wyputta (2003) to 25.5^{o}S, and

312　　show that Poaceae pollen percentages are between 30 and 40% offshore the Desert, Nama-Karoo

313　　and Fn-LSav biomes. As Poaceae pollen percentages in Desert surface samples are less than 25%,

314　　high percentages of grass pollen from marine sediments in the southwestern Africa margin should

315　　be interpreted as indicator of the Nama-Karoo and the Fn-LSav, where Poaceae is as high as 70% in

316　　terrestrial surface samples. Our field observations also support this view as we found large grass-

317　　dominated vegetation in the Nama-Karoo and Fn-LSav (Fig. 2).

318

319　　*4.3 Southwestern Africa vegetation and climatic changes from MIS 6 to 2*

320　　　　　The pollen record presented here spans from 24.7 to 190 ka. A log transformation of

321　　concentration values in MD96-2098 results in a curve remarkably similar to that of $\delta^{18}O_{benthic}$ values

322　　(Fig.4) and may be linked to changes in pollen input at the coring site. Relative increases in pollen

323　　concentration could indicate an increase in pollen supply during low sea-level stands when the

324　　vegetation source was closest (i.e. during glacial stages). However, this is unlikely because of the

325　　rapid depth change in a few kilometres of the Walvis continental shelf. An increase of pollen

326　　concentration might indicate instead an increase in pollen supply during glacials, and/or an increase

327　　in pollen preservation linked to upwelling enhancement as suggested by Pichevin et al. (2005).

328　　Glacial-interglacial pollen concentration variations have no effect on the interpretation of the pollen

329　　record which is based on relative frequencies, but they do indicate the influence of the obliquity

13

330 signal in the pollen record from MD96-2098. In other words, the effect of orbital-scale precipitation

331 changes on the density of the vegetation and the pollen production as a consequence.

332 The axis scores on DCA1 reveal changes in the composition of pollen assemblages that also

333 resemble variations in the $\delta^{18}O_{benthic}$ record (Fig.4). This similarity suggests that glacial-interglacial

334 vegetation changes in southern Africa track global ice volume changes. DCA1 axis scores from MIS 5

335 and 3 are overall positive in value, while scores from MIS 6 and 4 are negative, although clustering of

336 samples was not observed. The DCA1 axis represents relative changes in the pollen assemblage from

337 one sample to the next. A series of large-magnitude changes in DCA1 axis scores are also visible and

338 increase in amplitude after c. 100 ka. Such changes in DCA Axis1 scores are also observed during MIS

339 6 but are of lesser magnitude. Changes in DCA axis scores suggest significant changes in vegetation

340 composition from one sample to the next.

341 Nama-Karoo and Fn-LSav pollen percentages are up to 60% during MIS 5 and display three

342 percentage peaks that correspond with $\delta^{18}O_{benthic}$ and precession minima (Fig.4a). These percentage

343 peaks are centred at 125 ka, 107 and 83 ka. The pollen spectra from warm marine substages MIS 5e,

344 5c and 5a is comparable to the core-top samples (Fig. 4) and corresponds well with the modern

345 pollen spectra from Nama-Karoo and Fn-LSav (Fig. S3). Additionally, Nama-Karoo and Fn-LSav pollen

346 percentages in the core-top samples are relatively low compared to their maximum during MIS 5e

347 (Fig.4b).

348 During MIS 6 and 4, Nama-Karoo and Fn-LSav percentages are reduced and co-vary with

349 $\delta^{18}O_{benthic}$ values. Pollen percentages of Chenopodiaceae-Amaranthaceae and Asteraceae-other are

350 relatively high and increase along with enriched $\delta^{18}O_{benthic}$ values during MIS 6 and at the end of MIS

351 4 (Fig. S2). Cyperaceae pollen percentages vary throughout the record and are as high as 40% during

352 MIS 4 (Fig. S2). Fynbos indicators (Ericaceae, *Passerina*, *Anthospermum*, *Cliffortia*, and *Protea*

353 *Artemisa*-type and *Stoebe*-type) show relative increases in pollen percentage during MIS 6, 4 and 3

354 (Fig.4b and Fig. S2). Pollen percentages of Restionaceae increase after the 105-ka $\delta^{18}O_{benthic}$

355 minimum and remain abundant during the rest of MIS 5 through MIS 3, despite a relative decrease

14

356   during MIS 4. *Podocarpus* percentages are lower than 10% but show increases at stage boundaries

357   around 135 ka (MIS 6/5), 100 ka (5c/5b), 75 ka (MIS 5a/4), 60 ka (MIS 4/3), and around 27 ka (MIS

358   3/2) (Fig. S2).

359   The increases of Nama-Karoo and Fn-LSav during MIS 5e, 5c and 5a suggest an increase in

360   aridity in southwestern Africa that likely resulted from expansions in three directions (Fig. 5). The

361   Nama-Karoo and Fn-LSav probably expanded to the northwest into the present-day area of the

362   coastal Namib Desert as the intensity of BUS weakened during MIS 5 warm substages. This

363   weakening has been documented through alkenone-based SST from marine core GeoB1711-3 (Kirst

364   et al., 1999) (Fig.4c), foraminifera-assemblage based SST (Chen et al., 2002) and grain-size end-

365   member modelling (Stuut et al., 2002). Stuut and Lamy (2004) also suggested reduced atmospheric

366   circulation and weakening of trade winds during interglacials compared to glacials, resulting in a

367   reduction of the wind-driven upwelling. A weakened BUS and the associated relative increase in

368   humidity likely led to a colonization of Desert areas by Nama-Karoo or Fn-LSav (Fig.5a). Comparable

369   contractions of the Namib Desert linked to increased SSTs and weakening of BUS during the present

370   interglacial are documented by Shi et al. (2000).

371   To the south, the Nama-Karoo and Fn-LSav likely expanded at the expense of the Succulent-

372   Karoo and Fynbos. Warm Antarctica temperatures recorded during MIS 5 substages (EPICA, 2006)

373   would drive the southern westerlies southwards (Ruddiman, 2006), contributing to the ventilation of

374   deep CO_2-rich waters in the southern Ocean (Toggweiler and Russell, 2008). This mechanism would

375   explain the paralleling trends observed between MIS 5 Nama-Karoo and Fn-LSav expansions in

376   southern Africa and the atmospheric CO_2 record (Petit et al., 1999; Bereiter et al., 2012) (Fig.5). A

377   southward migration of the westerlies during the present interglacial, relative to their position

378   during the previous glacial, has been suggested by Weldeab et al. (2013), and correlated with non-

379   sea-salt calcium flux ($nssCa^{2+}$) from Antarctica (Röthlisberger et al., 2008). Such poleward migration

380   of the westerlies during the present interglacial is equivalent to the westerlies migration we propose

381   for warmest periods of the last interglacial. The increased Agulhas leakage documented in the Cape

382   basin record during the last interglacial (Peeters et al., 2004) (Fig.4c) has been linked to a southward

383   migration of the subtropical front and the westerlies, reducing austral-winter precipitation over

384   southern Africa. Such an atmospheric configuration would in turn favour the development of the

385   Nama-Karoo at the expense of Succulent-Karoo and Fynbos biomes (Fig.5a).

386   To the northeast, Nama-Karoo and Fn-LSav likely pushed the limit of Bd-LSav equatorward as

387   austral-summer precipitation decreased (Fig.5a). Austral-summer precipitation reductions in

388   southern Africa have been linked to reduced austral-summer insolation in the Pretoria saltpan

389   (Partridge et al., 1997) and to reductions of grass-fuelled fires during precession minima

390   reconstructed from MD96-2098 (Daniau et al., 2013) (Fig.4b). Increased northern-hemisphere

391   insolation during MIS 5 warm substages would drive the ITCZ northwards while subtropical high

392   pressure cells over the south Atlantic and the Indian Oceans would expand (Fig.5a) (Ruddiman,

393   2006). Such changes in the tropical and subtropical pressure systems would allow the expansion of

394   the Nama-Karoo and Fn-LSav to the northeast.

395   In contrast with the results presented here, previous works report poleward interglacial

396   expansions of savannas based on pollen records from marine sediments along the southwestern

397   African coast (Dupont, 2011). These studies univocally interpret the Poaceae pollen percentage

398   increases as the result of savanna expansions. Such an interpreation is potentially plausible in

399   marine records collecting pollen from broad-leaved savanna vegetation, e.g. the Limpopo basin

400   (Dupont, 2011). However, our results show that Poaceae pollen percentage increases in sequences

401   located off the southwestern African coast can alternatively indicate the expansion of fine-leaved

402   savanna and Nama-Karoo vegetation. Previous studies on the other hand do not differentiate

403   between the Bd-LSav and Fn-LSav, despite the significant climatic and structural differences between

404   these two types of vegetation. The Bd-LSav is influenced by fire and receives a considerable amount

405   of precipitation during the austral summer (Scholes, 1997). The Fn-LSav is structurally and

406   climatically more similar to the Nama-Karoo biome, as it receives very low austral-summer

407   precipitation and does not burn (Archibald et al., 2010) despite being under a regime of significant

408   precipitation seasonality (Scholes, 1997). If high Poaceae pollen percentages during MIS 5 warm

409   substages in our record were related with expansions of the Bd-LSav and increased summer

410   precipitation, the fire activity should also increase during these substages. Instead, an independent

411   charcoal record from the same marine sequence MD96-2098 (Fig.4b) documents reductions of

412   grass-fuelled fires and a decrease in austral-summer precipitation during MIS 5 precession minima

413   (Daniau et al., 2013). An atmospheric configuration with reduced austral summer precipitation in

414   southern Africa and the ITCZ shifted northward during the warmest periods of MIS 5 is also

415   consistent with documented strengthening of Asian monsoon and weakening of the South American

416   monsoon during the last-interglacial precession minima (Wang et al., 2004).

417   Our results suggest that the Bd-LSav retreated equatorwards during MIS 5 precession

418   minima, while Nama-Karoo and Fn-LSav expanded. Nama-Karoo and Fn-LSav probably covered a

419   surface area larger than at present during MIS 5 warm substages, as indicated by up to 70% pollen

420   from this biome during MIS 5 compared to 35% in the core-top samples. This is despite the

421   difference in precession parameters between the last millennium and MIS 5 warm substages. Recent

422   model experiments on the impact of precession changes on southern African vegetation indicate

423   that high precession is linked to reductions of the Bd-LSav (Woillez et al., 2014). Altogether these

424   vegetation changes point to increased aridity in southwestern Africa during the warmest periods of

425   the last interglacial.

426   During glacial isotopic stages, contractions of the Nama-Karoo and Fn-LSav would result

427   from a different atmospheric configuration (Fig.5b): a southward migration of the ITCZ and the

428   associated African monsoon (Daniau et al., 2013; Partridge et al., 1997) increasing austral-summer

429   rainfall over southern Africa; an intensification of BUS and decreased SST off the Namibian coast

430   (Stuut and Lamy, 2004; Kirst et al., 1999) leading to aridification of coastal areas; and lastly, an

431   equatorward migration of the westerlies increasing austral-winter precipitation and allowing a

432   northward expansion of the winter-rain zone in southern Africa (Chase and Meadows, 2007). The

433   proposed glacial precipitation changes are consistent with recent estimates of Last Glacial Maximum

434   palaeoprecipitation based on glacier reconstruction and mass-balance modelling (Mills et al., 2012),

435   with leaf-wax reconstructions of hydroclimate (Collins et al., 2014), and with simulated glacial

436   climatic fluctuations in southern Africa (Huntley et al., 2014).

437   The pollen record from MD96-2098 also suggested glacial expansions of Fynbos (Fig.4b), as

438   pollen percentages of *Artemisia*-type, *Stoebe*-type, *Passerina* and Ericaceae were higher during MIS

439   6, 4 and 3 than in the core-top samples (Fig. S2). These results were consistent with glacial

440   northward expansions of Fynbos documented in other pollen records from southern Africa (Shi et

441   al., 2000; Dupont et al., 2007). Our record also documented a large peak in Fynbos indicators (Fig.4b)

442   that coincided with a fast decrease in Nama-Karoo and fine-leaved savanna pollen percentages at

443   the MIS 5e/5d transition (c. 117 ka), a precession and eccentricity maxima (Laskar, 1990), and an

444   accelerated cooling in Antarctica (EPICA, 2006; Masson-Delmotte et al., 2010) (Fig.4c). As pollen

445   percentages of *Artemisia*-type obtained from surface samples were associated with the Fynbos

446   biome and austral-winter precipitation (Fig. S4 and S5), it cannot be discarded that this peak resulted

447   from a rapid and short-lived expansion of the winter-rain zone of southern Africa. Transitions MIS

448   6/5 and 4/3 were characterized by small but rapid increases in *Podocarpus*, potentially linked to a

449   short increase in annual precipitation. Such increases in *Podocarpus* have also been documented in

450   other records from southern Africa (Dupont, 2011).

451   Finally, the amplitude of millennial-scale vegetation changes increased between ca. 100 ka

452   and ca. 25 ka, and was highlighted by switches from negative to positive DCA1 scores (Fig.4b) and

453   increased variability of Restionaceae pollen percentages. Increased Restionaceae pollen could

454   indicate expansions of Fynbos vegetation, or enhanced pollen transport from the Fynbos region

455   linked to increased trade-wind strength (see additional discussion on present-day pollen-vegetation-

456   climate relationships in the Supplementary material). Other Fynbos indicators did not display the

457   same trend (Fig. 4), suggesting that Restionaceae variability between 100 ka and 24 ka were more

458   likely the result of enhanced variability of southeast trade winds. Restionaceae pollen percentage

459   data from a record two degrees of latitude north of our marine site also showed comparable

460 increases in the amplitude of millennial-scale changes (Shi et al., 2001). Grain-size wind strength

461 tracers from the Walvis Ridge also displayed enhanced millennial-scale variability, although only

462 after ca. 80 ka (Stuut and Lamy, 2004). An analysis of BUS dynamics over the past 190 ka found

463 increased millennial-scale variability of wind strength after ca. 100 ka and the highest wind strength

464 in this zone during MIS 4 and 3 (Stuut et al., 2002). Such millennial-scale atmospheric

465 reorganisations were probably recorded in the pollen-based DCA analysis as rapid biome shifts in

466 southwestern Africa.

467

468 **5. Conclusions**

469 Terrestrial and marine markers from the marine core MD96-2098 documented expansions

470 of the Nama-Karoo and fine-leaved savanna during MIS 5e, 5c and 5a warm substages.

471 Northwestern expansions of the Nama-Karoo and Fn-LSav are potentially linked to the reduction of

472 BUS and a local increase in humidity in the desert area, while aridification increased at a regional

473 scale. Towards the east, Nama-Karoo and Fn-LSav expansions probably resulted from increased

474 subtropical high pressure, a northward shift of the ITCZ, and reduced austral-summer precipitation.

475 Nama-Karoo and Fn-LSav expansions to the southern boundary are possibly associated with

476 southern displacement of the westerlies and the subtropical front, decreasing austral-winter

477 precipitation.

478 During glacial isotopic stages MIS 6, 4 and 3, Fynbos biome expansions are probably linked

479 to the increased influence of the southern westerlies and austral-winter precipitation in

480 southwestern Africa. Our pollen record also suggested that warm-cold or cold-warm transitions

481 between isotopic stages and substages were punctuated by short increases in humidity. Increased

482 variability of vegetation changes at millennial timescales ca. 100 ka was also documented and could

483 be associated with previously-identified enhanced variability of the southeastern trade winds.

484 Interglacial-glacial southern Africa biome dynamics were linked to atmospheric and oceanic

485 dynamics resulting from changes in global ice volume and precession at orbital timescales.

486   Atmospheric configurations with westerly winds shifted southwards relative to today have been

487   suggested for other interglacials (Peeters et al., 2004) and are projected for the end of 21st-century

488   under current global warming (Beal et al., 2011). This is likely to reduce austral-winter precipitation

489   over southern Africa and favour expansions of the Nama-Karoo at the expense of the winter-rain fed

490   Fynbos and Succulent-Karoo biomes. However, taking the current orbital configuration alone, the

491   Nama-Karoo and fine-leaved savanna in southern Africa might naturally remain relatively reduced

492   for several millennial ahead.

493

505

506   **References**

507 Archibald, S., Scholes, R. J., Roy, D. P., Roberts, G., and Boschetti, L.: Southern African fire regimes as
508 revealed by remote sensing, International Journal of Wildland Fire, 19, 861-878,
509 http://dx.doi.org/10.1071/WF10008, 2010.

510 Barnard, P.: Biological diversity in Namibia, The Namibian National Biodiversity Task Force,
511 Windhoek, Namibia, 332 pp., 1998.

512 Beal, L. M., and Bryden, H. L.: The velocity and vorticity structure of the Agulhas Current at 32°S,
513 Journal of Geophysical Research: Oceans, 104, 5151-5176, 10.1029/1998jc900056, 1999.

514 Beal, L. M., De Ruijter, W. P. M., Biastoch, A., and Zahn, R.: On the role of the Agulhas system in
515 ocean circulation and climate, Nature, 472, 429-436, 10.1038/nature09983, 2011.

516 Bereiter, B., Lüthi, D., Siegrist, M., Schüpbach, S., Stocker, T. F., and Fischer, H.: Mode change of
517 millennial CO2 variability during the last glacial cycle associated with a bipolar marine carbon
518 seesaw, Proceedings of the National Academy of Sciences, 109, 9755-9760,
519 10.1073/pnas.1204069109, 2012.

520 Bertrand, P., Balut, Y., Schneider, R., Chen, M. T., Rogers, J., and Shipboard Scientific Party: Scientific
521 report of the NAUSICAA-IMAGES II coring cruise. Les rapports de campagne à la mer à bord du
522 Marion-Dufresne, URA CNRS 197, Université Bordeaux1, Departement de Geologie et
523 Oceanographie, Talence, France, 382 pp, 1996.

524 Bertrand, P., Giraudeau, J., Malaize, B., Martinez, P., Gallinari, M., Pedersen, T. F., Pierre, C., and
525 Vénec-Peyré, M. T.: Occurrence of an exceptional carbonate dissolution episode during early glacial
526 isotope stage 6 in the Southeastern Atlantic, Marine Geology, 180, 235-248, 10.1016/s0025-
527 3227(01)00216-x, 2002.

528 Bertrand, P., Pedersen, T. F., Schneider, R., Shimmield, G., Lallier-Verges, E., Disnar, J. R., Massias, D.,
529 Villanueva, J., Tribovillard, N., Huc, A. Y., Giraud, X., Pierre, C., and Vénec-Peyre, M.-T.: Organic-rich
530 sediments in ventilated deep-sea environments: Relationship to climate, sea level, and trophic
531 changes, Journal of Geophysical Research, 108, 3045, 10.1029/2000JC000327, 2003.

532 Biastoch, A., Böning, C. W., and Lutjeharms, J. R. E.: Agulhas leakage dynamics affects decadal
533 variability in Atlantic overturning circulation, Nature, 456, 489-492, 2008.

534 Chase, B. M., and Meadows, M. E.: Late Quaternary dynamics of southern Africa's winter rainfall
535 zone, Earth-Science Reviews, 84, 103-138, http://dx.doi.org/10.1016/j.earscirev.2007.06.002, 2007.

536 Chen, M.-T., Chang, Y.-P., Chang, C.-C., Wang, L.-W., Wang, C.-H., and Yu, E.-F.: Late Quaternary sea-
537 surface temperature variations in the southeast Atlantic: a planktic foraminifer faunal record of the
538 past 600 000 yr (IMAGES II MD962085), Marine Geology, 180, 163-181, 10.1016/s0025-
539 3227(01)00212-2, 2002.

540 Collins, J. A., Schefuß, E., Govin, A., Mulitza, S., and Tiedemann, R.: Insolation and glacial–interglacial
541 control on southwestern African hydroclimate over the past 140 000 years, Earth and Planetary
542 Science Letters, 398, 1-10, http://dx.doi.org/10.1016/j.epsl.2014.04.034, 2014.

543 Cowling, R. M., Esler, K. J., Midgley, G. F., and Honig, M. A.: Plant functional diversity, species
544 diversity and climate in arid and semi-arid southern Africa, Journal of Arid Environments, 27, 141-
545 158, 1994.

546 Cowling, R. M., Richardson, D. M., and Mustart, P. J.: Fynbos, in: Vegetation of Southern Africa,
547 edited by: Cowling, R. M., Richardson, D. M., and Pierce, S. M., Cambridge University Press,
548 Cambridge, UK, 99-130, 1997a.

549 Cowling, R. M., Richardson, D. M., and Pierce, S. M.: Vegetation of Southern Africa, Cambridge
550 University Press, Cambridge, UK, 615 pp., 1997b.

551 Cowling, R. M., and Hilton-Taylor, C.: Phytogeography, flora and endemism, in: The Karoo. Ecological
552 Patterns and Processes, edited by: Dean, W. R. J., and Milton, S., Cambridge University Press,
553 Cambridge, UK, 42-56, 2009.

554 Daniau, A.-L., Sánchez Goñi, M. F., Martinez, P., Urrego, D. H., Bout-Roumazeilles, V., Desprat, S., and
555 Marlon, J. R.: Orbital-scale climate forcing of grassland burning in southern Africa, Proceedings of the
556 National Academy of Sciences, 110, 5069–5073, 10.1073/pnas.1214292110, 2013.

557 Dewar, G., Reimer, P. J., Sealy, J., and Woodborne, S.: Late-Holocene marine radiocarbon reservoir
558 correction (ΔR) for the west coast of South Africa, The Holocene, 22, 1481-1489,
559 10.1177/0959683612449755, 2012.

560 Drysdale, R. N., Zanchetta, G., Hellstrom, J. C., Fallick, A. E., McDonald, J., and Cartwright, I.:
561 Stalagmite evidence for the precise timing of North Atlantic cold events during the early last glacial,
562 Geology, 35, 77-80, 2007.

563 Dupont, L. M., and Wyputta, U.: Reconstructing pathways of aeolian pollen transport to the marine
564 sediments along the coastline of SW Africa, Quaternary Science Reviews, 22, 157-174, 2003.

565 Dupont, L. M., and Behling, H.: Land–sea linkages during deglaciation: High-resolution records from
566 the eastern Atlantic off the coast of Namibia and Angola (ODP site 1078), Quaternary International,
567 148, 19-28, 10.1016/j.quaint.2005.11.004, 2006.

568 Dupont, L. M., Behling, H., Jahns, S., Marret, F., and Kim, J.-H.: Variability in glacial and Holocene
569 marine pollen records offshore from west southern Africa, Vegetation History and Archaeobotany,
570 16, 87-100, 10.1007/s00334-006-0080-8, 2007.

571 Dupont, L. M.: Orbital scale vegetation change in Africa, Quaternary Science Reviews, 30, 3589-3602,
572 10.1016/j.quascirev.2011.09.019, 2011.

573 EPICA: One-to-one coupling of glacial climate variability in Greenland and Antarctica, Nature, 444,
574 195-198, 10.1038/nature05301, 2006.

575 Faegri, K., and Iversen, J.: Textbook of Pollen Analysis, 4th ed., Wiley, Chichester, 328 pp., 1989.

576 Goldblatt, P.: An Analysis of the Flora of Southern Africa: Its Characteristics, Relationships, and
577 Orgins, Annals of the Missouri Botanical Garden, 65, 369-436, 10.2307/2398858, 1978.

578 González, C., and Dupont, L. M.: Tropical salt marsh succession as sea-level indicator during Heinrich
579 events, Quaternary Science Reviews, 28, 939-946, 10.1016/j.quascirev.2008.12.023, 2009.

580 Govin, A., Holzwarth, U., Heslop, D., Ford Keeling, L., Zabel, M., Mulitza, S., Collins, J. A., and Chiessi,
581 C. M.: Distribution of major elements in Atlantic surface sediments (36 N–49 S): Imprint of
582 terrigenous input and continental weathering, Geochemistry, Geophysics, Geosystems, 13, Q01013,
583 2012.

584 Henderson, G. M., and Slowey, N. C.: Evidence from U-Th dating against Northern Hemisphere
585 forcing of the penultimate deglaciation, Nature, 404, 61-66, 10.1038/35003541, 2000.

586 Heusser, L., and Balsam, W. L.: Pollen distribution in the northeast Pacific Ocean, Quaternary
587 Research, 7, 45-62, 10.1016/0033-5894(77)90013-8, 1977.

588 Hooghiemstra, H., Agwu, C. O. C., and Beug, H.-J.: Pollen and spore distribution in recent marine
589 sediments: a record of NW-African seasonal wind patterns and vegetation belts, Meteor Forschungs-
590 Ergebnisse C, 40, 87-135, 1986.

591 Hooghiemstra, H., Stalling, H., Agwu, C. O. C., and Dupont, L. M.: Vegetational and climatic changes
592 at the northern fringe of the Sahara 250,000–5000 years BP: evidence from 4 marine pollen records
593 located between Portugal and the Canary Islands, Review of Palaeobotany and Palynology, 74, 1-53,
594 10.1016/0034-6667(92)90137-6, 1992.

595 Hughen, K., Baillie, M., Bard, E., Bayliss, A., Beck, J., Bertrand, C., Blackwell, P., Buck, C., Burr, G.,
596 Cutler, K., Damon, P., Edwards, R., Fairbanks, R., Friedrich, M., Guilderson, T., Kromer, B., McCormac,
597 F., Manning, S., Ramsey, C. B., Reimer, P., Reimer, R., Remmele, S., Southon, J., Stuiver, M., Talamo,
598 S., Taylor, F., Plicht, J. v. d., and Weyhenmeyer, C.: Marine04 Marine radiocarbon age calibration, 26
599 - 0 ka BP, Radiocarbon, 46, 1059-1086, 2004.

600 Huntley, B., Midgley, G. F., Barnard, P., and Valdes, P. J.: Suborbital climatic variability and centres of
601 biological diversity in the Cape region of southern Africa, Journal of Biogeography, 41, 1338-1351,
602 2014.

603 Imhoff, M. L., Bounoua, L., Ricketts, T., Loucks, C., Harriss, R., and Lawrence, W. T.: Global patterns in
604 human consumption of net primary production, Nature, 429, 870-873, 2004.

605 IPCC: Fifth Assessment Report of the Intergovernmental Panel on Climate Change,
606 Intergovernmental Panel on Climate Change, NJ, USA, 2014.

607 Jürgens, N., Burke, A., Seely, M. K., and Jacobson, K. M.: Desert, in: Vegetation of Southern Africa,
608 edited by: Cowling, R. M., Richardson, D. M., and Pierce, S. M., Cambridge Unversity Press,
609 Cambridge, 189-214, 1997.

610 Kirst, G. J., Schneider, R. R., Müller, P. J., von Storch, I., and Wefer, G.: Late Quaternary temperature
611 variability in the Benguela Current System derived from alkenones, Quaternary Research, 52, 92-
612 103, 10.1006/qres.1999.2040, 1999.

613 Laskar, J.: The chaotic motion of the solar system: A numerical estimate of the chaotic zones, Icarus,
614 88, 266-291, 1990.

615 Leroy, S., and Dupont, L.: Development of vegetation and continental aridity in northwestern Africa
616 during the Late Pliocene: the pollen record of ODP site 658, Palaeogeography, Palaeoclimatology,
617 Palaeoecology, 109, 295-316, 10.1016/0031-0182(94)90181-3, 1994.

618 Lézine, A., and Hooghiemstra, H.: Land-sea comparisons during the last glacial-interglacial transition:
619 pollen records from West Tropical Africa, Palaeogeography, Palaeoclimatology, Palaeoecology, 79,
620 313-331, 10.1016/0031-0182(90)90025-3, 1990.

621 Lisiecki, L. E., and Raymo, M. E.: A Pliocene-Pleistocene stack of 57 globally distributed benthic d18O
622 records, Paleoceanography, 20, PA1003, 10.1029/2004pa001071, 2005.

623 Lutjeharms, J. R. E., and Meeuwis, J. M.: The extent and variability of South-East Atlantic upwelling,
624 South African Journal of Marine Science, 5, 51-62, 10.2989/025776187784522621, 1987.

625 Lyle, M., Heusser, L., Ravelo, C., Yamamoto, M., Barron, J., Diffenbaugh, N. S., Herbert, T., and
626 Andreasen, D.: Out of the tropics: the Pacific, Great Basin Lakes, and Late Pleistocene water cycle in
627 the western United States, Science, 337, 1629-1633, 2012.

628 Masson-Delmotte, V., Stenni, B., Pol, K., Braconnot, P., Cattani, O., Falourd, S., Kageyama, M., Jouzel,
629 J., Landais, A., Minster, B., Barnola, J. M., Chappellaz, J., Krinner, G., Johnsen, S., Röthlisberger, R.,
630 Hansen, J., Mikolajewicz, U., and Otto-Bliesner, B.: EPICA Dome C record of glacial and interglacial
631 intensities, Quaternary Science Reviews, 29, 113-128, 2010.

632 McCune, B., and Grace, J. B.: Analysis of ecological communities, MjM Software Design, Gleneden
633 Beach, Oregon, 300 pp., 2002.

634 Meadows, M. E., Chase, B. M., and Seliane, M.: Holocene palaeoenvironments of the Cederberg and
635 Swartruggens mountains, Western Cape, South Africa: Pollen and stable isotope evidence from
636 hyrax dung middens, Journal of Arid Environments, 74, 786-793,
637 http://dx.doi.org/10.1016/j.jaridenv.2009.04.020, 2010.

638 Mills, S. C., Grab, S. W., Rea, B. R., Carr, S. J., and Farrow, A.: Shifting westerlies and precipitation
639 patterns during the Late Pleistocene in southern Africa determined using glacier reconstruction and
640 mass balance modelling, Quaternary Science Reviews, 55, 145-159,
641 http://dx.doi.org/10.1016/j.quascirev.2012.08.012, 2012.

642 Milton, S. J., Yeaton, R. I., Dean, W. R. J., and Vlok, J. H. J.: Succulent karoo, in: Vegetation of
643 Southern Africa, edited by: Cowling, R. M., Richardson, D. M., and Pierce, S. M., Cambridge Unversity
644 Press, Cambridge, 131-166, 1997.

645 O'Connor, T. G., and Bredenkamp, G. J.: Grassland, in: Vegetation of Southern Africa, edited by:
646 Cowling, R. M., Richardson, D. M., and Pierce, S. M., Cambridge University Press, Cambridge, UK,
647 215-257, 1997.

648 Palmer, A. R., and Hoffman, M. T.: Nama-Karoo, in: Vegetation of Southern Africa, edited by:
649 Cowling, R. M., Richardson, D. M., and Pierce, S. M., Cambridge Unversity Press, Cambridge, 167-
650 188, 1997.

651 Partridge, T. C., Demenocal, P. B., Lorentz, S. A., Paiker, M. J., and Vogel, J. C.: Orbital forcing of
652 climate over South Africa: A 200,000-year rainfall record from the pretoria saltpan, Quaternary
653 Science Reviews, 16, 1125-1133, http://dx.doi.org/10.1016/S0277-3791(97)00005-X, 1997.

654 Peeters, F. J. C., Acheson, R., Brummer, G.-J. A., de Ruijter, W. P. M., Schneider, R. R., Ganssen, G. M.,
655 Ufkes, E., and Kroon, D.: Vigorous exchange between the Indian and Atlantic oceans at the end of
656 the past five glacial periods, Nature, 430, 661-665, 10.1038/nature02785, 2004.

657 Petit, J. R., Jouzel, J., Raynaud, D., Barkov, N. I., Barnola, J.-M., Basile, I., Bender, M., and Chappellaz,
658 J.: Climate and atmospheric history of the past 420,000 years from the Vostok ice core, Antarctica,
659 Nature, 399, 429-436, 1999.

660 Pichevin, L., Martinez, P., Bertrand, P., Schneider, R., Giraudeau, J., and Emeis, K.: Nitrogen cycling on
661 the Namibian shelf and slope over the last two climatic cycles: Local and global forcings,
662 Paleoceanography, 20, PA2006, 10.1029/2004pa001001, 2005.

663 Reimer, P. J., Bard, E., Bayliss, A., Beck, J. W., Blackwell, P. G., Bronk Ramsey, C., Buck, C. E., Cheng,
664 H., Edwards, R. L., Friedrich, M., Grootes, P. M., Guilderson, T. P., Haflidason, H., Hajdas, I., Hatté, C.,
665 Heaton, T. J., Hoffmann, D. L., Hogg, A. G., Hughen, K. A., Kaiser, K. F., Kromer, B., Manning, S. W.,
666 Niu, M., Reimer, R. W., Richards, D. A., Scott, E. M., Southon, J. R., Staff, R. A., Turney, C. S. M., and
667 Plicht, J. v. d.: IntCal13 and Marine13 radiocarbon age calibration curves 0-50,000 years cal BP,
668 Radiocarbon, 55, 1869-1887, 2013.

669 Rogers, J., and Rau, A. J.: Surficial sediments of the wave-dominated Orange River Delta and the
670 adjacent continental margin off south-western Africa, African Journal of Marine Science, 28, 511-
671 524, 10.2989/18142320609504202, 2006.

672 Röthlisberger, R., Mudelsee, M., Bigler, M., De Angelis, M., Fischer, H., Hansson, M., Lambert, F.,
673 Masson-Delmotte, V., Sime, L., and Udisti, R.: The Southern Hemisphere at glacial terminations:
674 insights from the Dome C ice core, Climate of the Past, 4, 345-356, 2008.

675 Ruddiman, W. F.: Orbital changes and climate, Quaternary Science Reviews, 25, 3092-3112, 2006.

676 Rutherford, M. C.: Categorization of biomes, in: Vegetation of Southern Africa, edited by: Cowling, R.
677 M., Richardson, D. M., and Pierce, S. M., Cambridge University Press, Cambridge, UK, 91-98, 1997.

678 Sánchez Goñi, M. F., Eynaud, F., Turon, J. L., and Shackleton, N. J.: High resolution palynological
679 record off the Iberian margin: direct land-sea correlation for the Last Interglacial complex, Earth and
680 Planetary Science Letters, 171, 123-137, 10.1016/s0012-821x(99)00141-7, 1999.

681 Sánchez Goñi, M. F., Turon, J.-L., Eynaud, F., and Gendreau, S.: European climatic response to
682 millennial-scale changes in the atmosphere–ocean system during the Last Glacial period, Quaternary
683 Research, 54, 394-403, 10.1006/qres.2000.2176, 2000.

684 Sánchez Goñi, M. F., and Harrison, S. P.: Millennial-scale climate variability and vegetation changes
685 during the Last Glacial: Concepts and terminology, Quaternary Science Reviews, 29, 2823-2827,
686 2010.

687 Scholes, R. J.: Savanna, in: Vegetation of Southern Africa, edited by: Cowling, R. M., Richardson, D.
688 M., and Pierce, S. M., Cambridge University Press, Cambridge, UK, 258-277, 1997.

689   Scott, L.: Late Quaternary fossil pollen grains from the Transvaal, South Africa, Review of
690   Palaeobotany and Palynology, 36, 241-268, 1982.

691   Scott, L., Marais, E., and Brook, G. A.: Fossil hyrax dung and evidence of Late Pleistocene and
692   Holocene vegetation types in the Namib Desert, Journal of Quaternary Science, 19, 829-832,
693   10.1002/jqs.870, 2004.

694   Scott, L., Neumann, F. H., Brook, G. A., Bousman, C. B., Norström, E., and Metwally, A. A.: Terrestrial
695   fossil-pollen evidence of climate change during the last 26 thousand years in Southern Africa,
696   Quaternary Science Reviews, 32, 100-118, http://dx.doi.org/10.1016/j.quascirev.2011.11.010, 2012.

697   Shi, N., Dupont, L. M., Beug, H.-J., and Schneider, R.: Correlation between vegetation in
698   southwestern Africa and oceanic upwelling in the past 21,000 years, Quaternary Research, 54, 72-80,
699   10.1006/qres.2000.2145, 2000.

700   Shi, N., Schneider, R., Beug, H.-J., and Dupont, L. M.: Southeast trade wind variations during the last
701   135 kyr: evidence from pollen spectra in eastern South Atlantic sediments, Earth and Planetary
702   Science Letters, 187, 311-321, 10.1016/s0012-821x(01)00267-9, 2001.

703   Southon, J., Kashgarian, M., Fontugne, M., Metivier, B., and Yim, W. W.-S.: Marine reservoir
704   corrections for the Indian Ocean and Southeast Asia, Radiocarbon 44, 167-180, 2002.

705   Stuut, J.-B. W., Prins, M. A., Schneider, R. R., Weltje, G. J., Jansen, J. H. F., and Postma, G.: A 300-kyr
706   record of aridity and wind strength in southwestern Africa: inferences from grain-size distributions
707   of sediments on Walvis Ridge, SE Atlantic, Marine Geology, 180, 221-233, 10.1016/s0025-
708   3227(01)00215-8, 2002.

709   Stuut, J.-B. W., and Lamy, F.: Climate variability at the southern boundaries of the Namib
710   (southwestern Africa) and Atacama (northern Chile) coastal deserts during the last 120,000 yr,
711   Quaternary Research, 62, 301-309, http://dx.doi.org/10.1016/j.yqres.2004.08.001, 2004.

712   Toggweiler, J. R., and Russell, J.: Ocean circulation in a warming climate, Nature, 451, 286-288, 2008.

713   Tyson, P. D.: Atmospheric circulation changes and palaeoclimates of southern Africa, South African
714   Journal of Science, 95, 194-201, 1999.

715   Tyson, P. D., and Preston-Whyte, R. A.: The weather and climate of southern Africa, Oxford
716   University Press Southern Africa, Cape Town, 396 pp., 2000.

717   Waelbroeck, C., Frank, N., Jouzel, J., Parrenin, F., Masson-Delmotte, V., and Genty, D.: Transferring
718   radiometric dating of the last interglacial sea level high stand to marine and ice core records, Earth
719   and Planetary Science Letters, 265, 183-194, 2008.

720   Wang, X., Auler, A. S., Edwards, R. L., Cheng, H., Cristalli, P. S., Smart, P. L., Richards, D. A., and Shen,
721   C.-C.: Wet periods in northeastern Brazil over the past 210 kyr linked to distant climate anomalies,
722   Nature, 432, 740-743, 2004.

723   Weldeab, S., Stuut, J.-B. W., Schneider, R. R., and Siebel, W.: Holocene climate variability in the
724   winter rainfall zone of South Africa, Climate of the Past, 9, 2347-2364, 10.5194/cp-9-2347-2013,
725   2013.

726   White, F.: The vegetation of Africa: a descriptive memoir to accompany the Unesco/AETFAT/UNSO
727   vegetation map of Africa, Paris, 356, 1983.

728   Woillez, M. N., Levavasseur, G., Daniau, A. L., Kageyama, M., Urrego, D. H., Sánchez-Goñi, M. F., and
729   Hanquiez, V.: Impact of precession on the climate, vegetation and fire activity in southern Africa
730   during MIS4, Climate of the Past, 10, 1165-1182, 10.5194/cp-10-1165-2014, 2014.

731

732
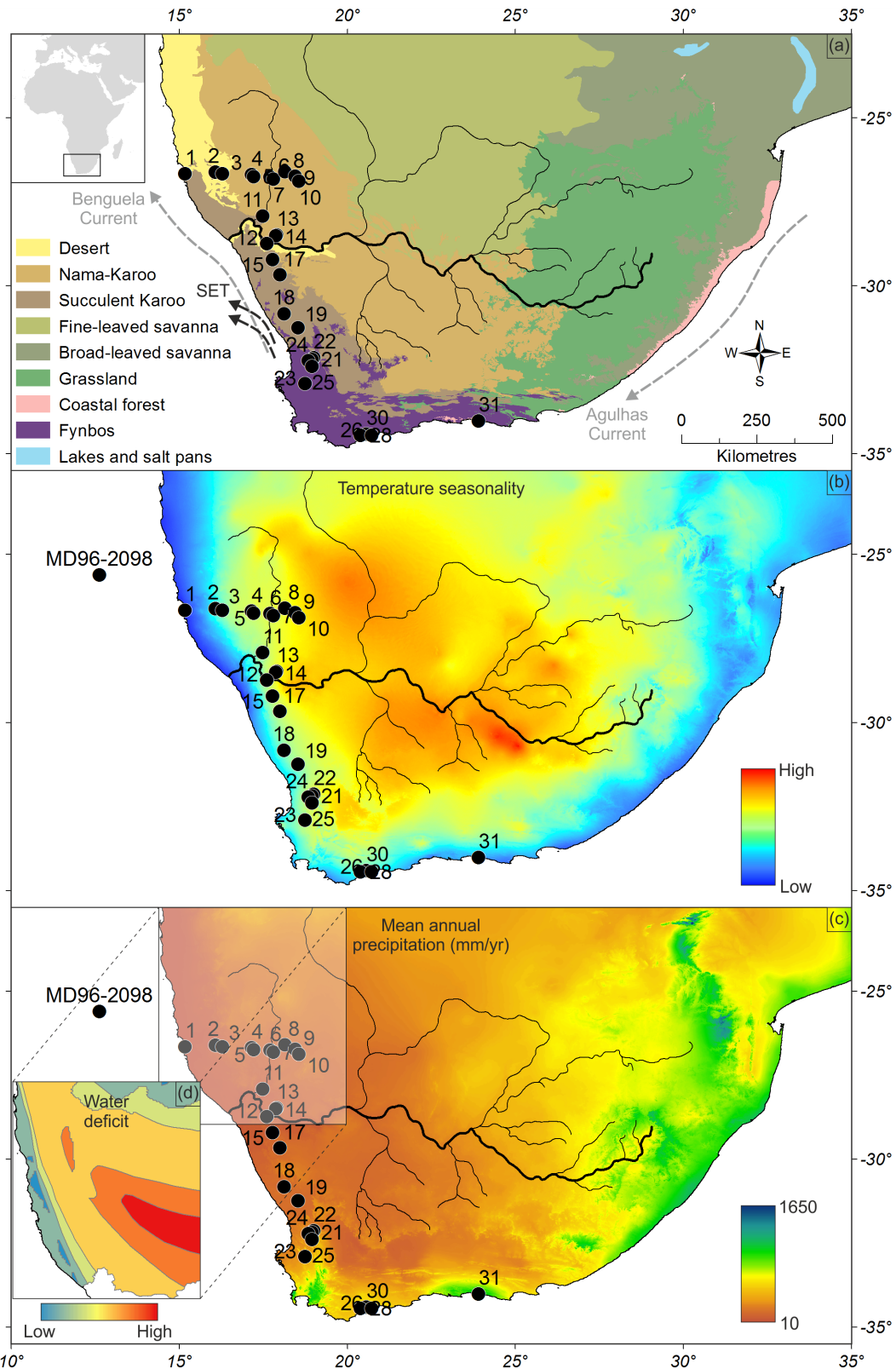
Figure 1. (a) Map of biomes of southern Africa based on Mucina et al. (2007) and modified using the savanna classification by Scholes (1997), location of the Orange River and major tributaries, oceanic currents (grey arrows) and southeastern trade winds (black arrows). Temperature seasonality (b) and annual precipitation in mm yr^{-1} (c) extracted from the WorldClim dataset (Hijmans et al., 2005). Water deficit data (c) redrawn from Barnard (1998) and Digital Atlas of Namibia (http://www.uni-koeln.de/sfb389/e/e1/download/atlas_namibia).

740   Black dots indicate location of marine core MD96-2098 and numbers indicate the location
741   of surface sample collection points described in Table S1.
742
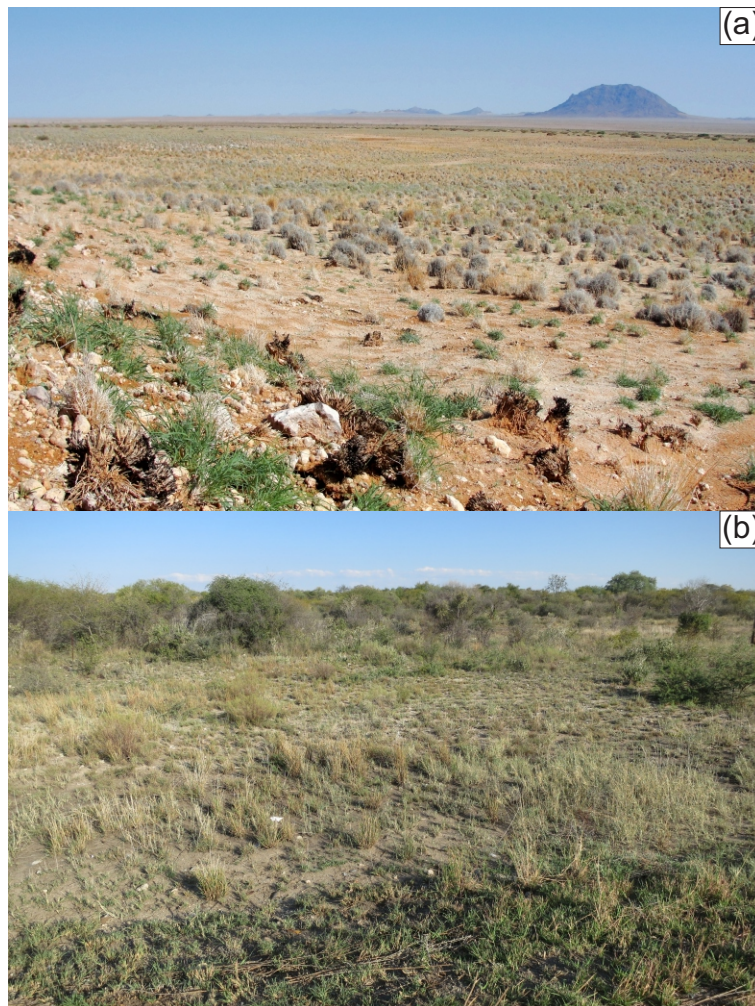
743
744   **Figure 2.** (a) Grass-dominated Nama-Karoo vegetation near Grunau, Namibia. Photo: D.H. Urrego.
745   (b) Grass-dominated fine-leaved savanna vegetation in the Kalahari region of Namibia. Photo: F.
746   D'Errico.
747
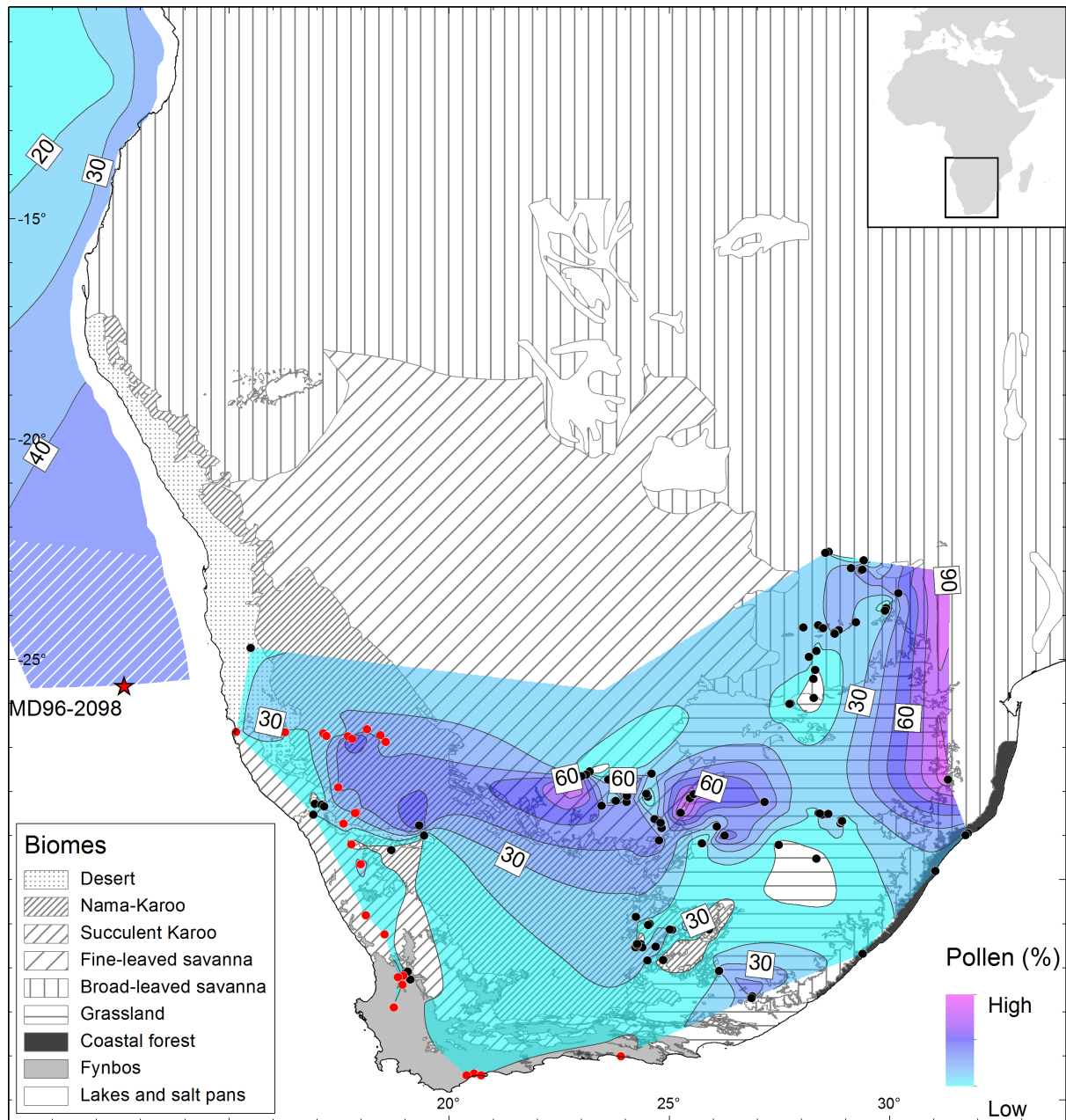
Figure 3. Poaceae pollen percentage iso-lines drawn over biome units of southern Africa (modified from Scholes (1997); Mucina et al., (2007)). The broad-leaved savanna distribution includes the Mopane and mixed savannas described by Scholes (1997). Iso-lines are plotted based on pollen percentage data from surface samples analysed in this study (red dots) and pollen spectra from other samples previously published and extracted from the African Pollen Database (black dots) (Gajewski et al., 2002). Poaceae pollen percentage in the marine domain are redrawn from Dupont and Wyputta (2003) and extended to latitude 25°S using two MD96-2098 core-top samples (hatched).
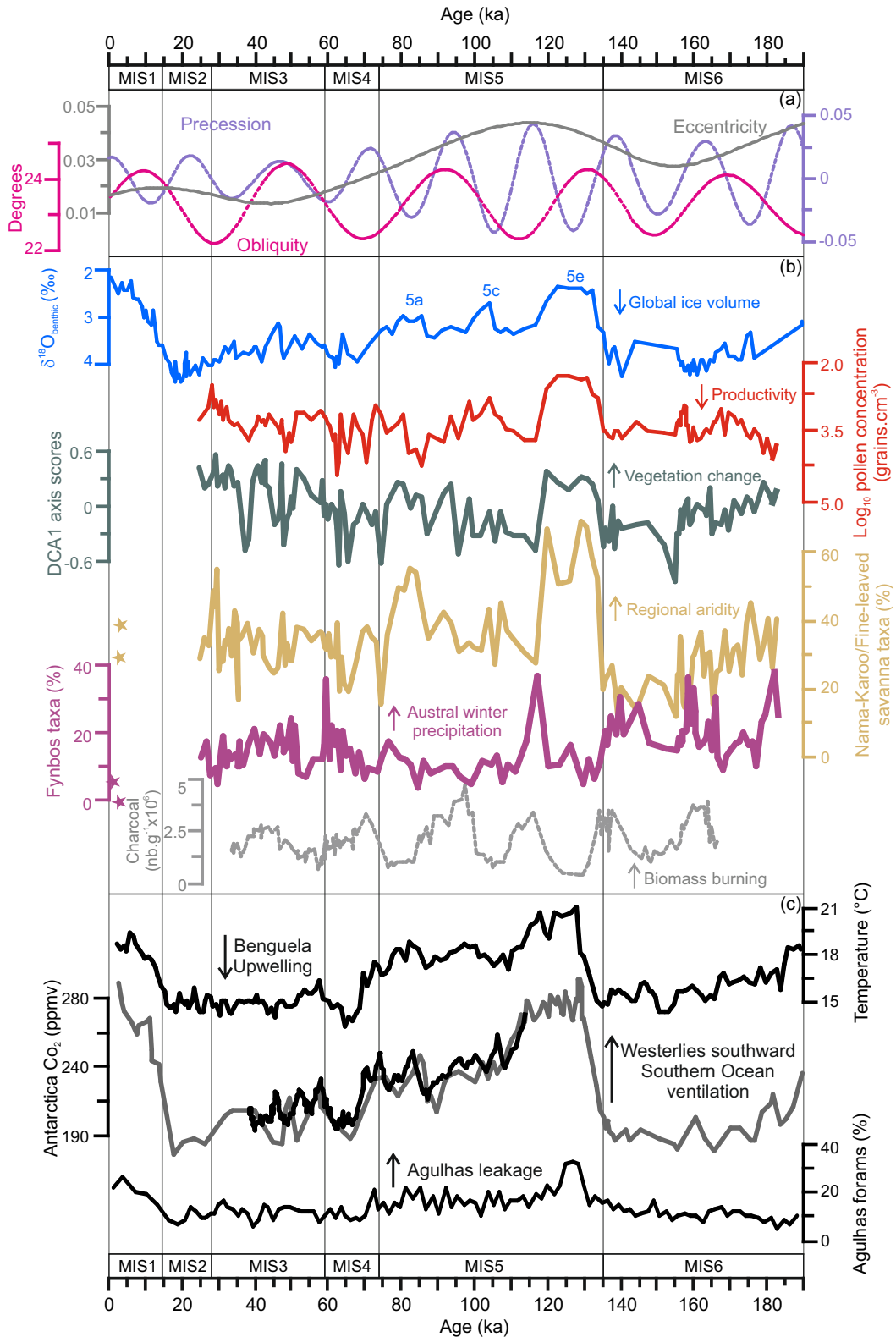
Figure 4. Terrestrial, atmospheric and oceanic markers from southern Africa plotted against age in ka (thousands of calibrated/calendar years before present). (a) Orbital parameters plotted for latitude 25°36'S using La2004 (Laskar et al., 2004). (b) Stable Oxygen profile of benthic foraminifera *Cibicidoides wuellerstorfi* (Bertrand et al., 2002), log-transformed total pollen concentration plotted on an descending scale, detrended correspondence analysis Axis1 scores, pollen percentages of indicator taxa for Nama-Karoo and fine-leaved savanna (Acanthaceae, Aizoaceae, Crassulaceae, Euphoria, Poaceae, and *Tribulus*,) and Fynbos (*Artemisia*-type,

Ericaceae, Passerina, *Protea*, and *Stoebe*-type), charcoal concentrations in number of particles per gram (nb.g^{-1}) from marine core MD96-2098 indicating biomass burning (Daniau et al., 2013). Stars on the left correspond to percentage of pollen taxa in two top-core samples dating 530 and 1060 calibrated years before present. (c) Independent climatic records discussed in the text: Alkenone-based SST record from GeoB1711-3 indicating the strength of the Benguela Upwelling system (Kirst et al., 1999), Antarctica CO2 record, gray curve: low-resolution record from Vostok (Petit et al., 1999); black curve: high-resolution EDML-Talos Dome Antarctic Ice Core CO$_2$ data (Bereiter et al., 2012), and Cape Basin spliced record of planktic foraminifera assemblages indicating the strength of the Agulhas leakage (Peeters et al., 2004). Stage boundary ages for 3/2, 4/3, and 5/4 from (Sanchez Goñi and Harrison, 2010) and 6/5 from (Henderson and Slowey, 2000).
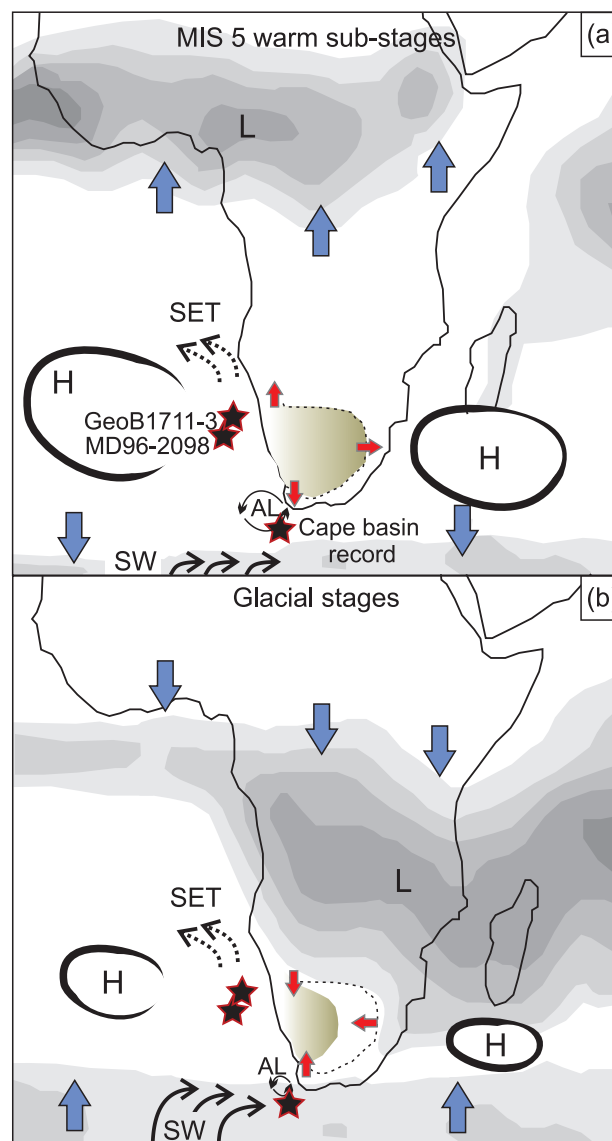
Figure 5. Schematic and simplified configuration of vegetation, atmospheric, and oceanic systems over southern Africa during (a) the MIS 5 warm substages, and (b) glacial isotopic stages. Rainfall is illustrated as grey areas showing the current configuration of tropical and subtropical convection systems using average austral-winter (a) and austral-summer (b) precipitation data between 1979–1995 from the International Research Institute for Climate Prediction (http://iri.ldeo.columbia.edu). L: tropical low-pressure systems, H: subtropical high-pressure systems, SET: southeast trade winds, SW: southern westerlies, AL: Agulhas leakage. Stars indicate the location of marine records discussed in the text and

787   blue arrows indicate the direction of pressure system migration. Red arrows and brown
788   shaded area indicate hypothesized expansion (a) or contraction of the Nama-Karoo and
789   fine-leaved savanna (b).
790